Proceedings of the 16th International Conference on System Theory, Control and Computing
Sinaia, Romania, October 12-14, 2012
IEEE Catalog Number CFP1236P-CDR, ISBN 978-606-834-848-3

Predictive Control of Anaerobic Digestion of Wastewater Sludge.
A Feasibility Study

Anamaria Ordace, Clara M. Ionescu, *Member, IEEE,* Thomas P.W. Vannecke, Eveline I.P. Volcke, Ioan Nascu and Robin De Keyser

***Abstract*— This paper presents the analysis, modeling, identification and predictive control of an anaerobic digestion process. The widely adopted anaerobic digestion model ADM1 is used to describe the anaerobic digestion of primary and secondary wastewater sludge. Their feed flow rates constitute two model inputs, which are considered as manipulated variables, while the biogas production rate and its methane content constitute two model outputs (controlled variables). The general control objective is to manipulate the inputs within the operation limits such that a maximum methane production is ensured at all times. A comparison between open-loop and closed-loop control reveals the net advantage of predictive control for optimal rate regulation.**

I. Introduction

Anaerobic Digestion is a complex biological process carried out in the absence of oxygen that involves hundreds of different types of microorganisms, which break down biodegradable organic matter. It is typically applied for the treatment of sewage sludge produced during municipal wastewater treatment, but it can also be applied to other waste (water) streams or non-waste feedstocks. Anaerobic digestion reduces the Chemical Oxygen Demand (COD) of the influent and produces valuable energy in the form of biogas, a mixture of mainly methane and carbon dioxide. The production of a clean, renewable energy constitutes the main advantage of the anaerobic digestion and gave rise to its increasing popularity in the last few years. Even though anaerobic digestion processes have been applied for over hundred years, there is still a large potential for advanced control techniques to widen the competitive scope of this process [1].

Several advanced control strategies have been developed (see [1] for an overview). Previous control strategies vary from rule-based expert database [2], fuzzy control [3] and adaptive polynomial control functions [4]. These control strategies are limited to the analysis of the past dynamics to decide upon the future control efforts. However, it is well-known that such processes where advanced control may have a significant impact on the overall efficiency and optimality of the plant operation are suitable for predictive control algorithms. These model based predictive controllers (MPC) take into account not only the past information, but also predictions of the future behavior of the system, optimizing thus the control effort over an interval of future control inputs. Although predictive control has already been applied to wastewater treatment processes [5],[6],[7], to the author's best knowledge it has not yet been used to control the anaerobic digestion process. In this study, a predictive control strategy developed at Ghent University [8] is tested on the anaerobic digestion process to verify whether or not predictive control can bring an added value to the state of art in anaerobic digestion process control.

This paper is structured as follows: the benchmark is briefly described in the next section, followed by a dynamic and static analysis in section III. The identification and model validation is done in section IV, while the principles of predictive control are given in section V. The results of open-loop control are compared with those for predictive control in section VI, followed by conclusions and perspectives for research in this direction.

II. Model Description – Control Objectives

In this study, the widely adopted Anaerobic Digestion Model No. 1 (ADM1) proposed by the IWA Task Group for Mathematical Modeling of Anaerobic Digestion Processes [9],[10] is used to describe the anaerobic digestion process of primary and secondary sludge from wastewater treatment.

The anaerobic digester is used for the treatment of the solids discarded from the primary clarifier and the thickened sludge originated from the secondary clarifier. The characteristics of the primary and secondary sludge streams are clearly different in terms of the strength and biodegradability [11]. For instance, the percentage of total suspended solids (TSS) in the underflow of the primary clarifier (primary sludge) is 3%, while it amounts to 7% in the underflow of the thickener (secondary sludge). Moreover, the sludge thickened from the bottom of the secondary clarifier has been already exposed to a biological treatment for nitrogen removal while the only procedure inflicted on the influent wastewater for the primary sludge is a gravitational settling.

The ADM1 model from Fig. 1 has been extended in order to have a multivariable setup. The manipulated variables ($q_{Thickener}$; $q_{Primary}$) are considered as explicit inputs in the anaerobic digester ADM1.

A. Ordace and I. Nascu are with Technical University of Cluj-Napoca, Department of Automation and Control Engineering, Cluj, Romania. The results presented in this paper have been obtained during an exchange study at Ghent University, Department of Electrical energy, Systems and Automation, Gent; Belgium. (e-mail: aordace@yahoo.com)

C.M. Ionescu and R. De Keyser are with Ghent University, Department of Electrical energy, Systems and Automation, Technologiepark 913, Gent-Zwijnaarde, 9052, Belgium. (e-mail: claramihaela.ionescu@ugent.be; robain.dekeyser@ugent.be). Clara Ionescu is supported by the Research Foundation-Flanders (FWO) through a Post-Doc fellowship

T.P.W. Vannecke and E.I.P. Volcke are with Ghent University, Department of Biosystems Engineering, Coupure Links 653, B-9000 Gent, Belgium (e-mail: thomas.vannecke@UGent.be, eveline.volcke@ugent.be). Thomas Vannecke is supported by the Research Foundation-Flanders (FWO) through a Ph.D. fellowship.

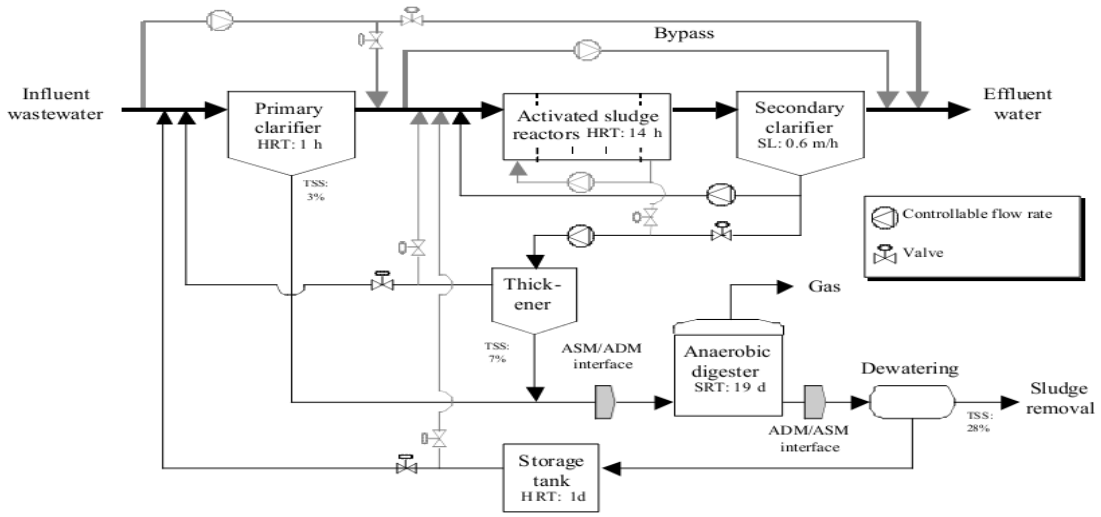

Figure 1. Schematic overview of the full BSM2 benchmark simulator [7]; notice the anaerobic digester block in the scheme with one input and 2 outputs. In this paper, we use a modified version of the ADM1, namely we consider 2 buffers for clarifier and thickener as manipulated variables.

The data of the two inputs of the ADM1 are obtained by simulating the BSM2 (Benchmark Simulation No. 2) plant in closed loop without water recirculation such that the ammonium load of the influent will not be violated. Another option is to use a SHARON-Anammox process as described in [12]. The dynamic influent data includes a reasonable amount of infiltration, rain, transformation of sewers etc. Two sets of input files are created: the constant values influents file used for the model identification and the dynamic influents data file used for testing the control strategy. The first set consists actually of the final values of the two influents of the anaerobic digester obtained by simulating the BSM2 plant in feed with constant composition for 10000 samples. The second set contains data sampled at 15 minutes of the concerning influents, when the BSM2 plant is simulated with full dynamic influent data for 609 days.

The control objective concerns the maximization of the methane production (kgCOD.m-3). However, this variable of interest cannot be measured directly – given that the produced biogas consists of carbon dioxide, besides methane – but is the product between the biogas flow rate $q_{gas}\left(\frac{m^3}{d}\right)$ and the methane concentration in biogas $S_{gas,CH_4}\left(\frac{kgCOD}{m^3}\right)$. The overall objective consists in the optimization of methane production while keeping the process stable by manipulating the flow rate of the two input streams coming from Thickener and from Primary Clarifier, as shown in Fig. 2. It has been assumed now that the flows can be adjusted freely. However in reality all primary and secondary sludge needs to be treated – even though temporary storage may be foreseen (buffer tank).

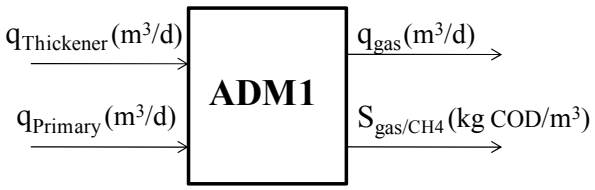

Figure 2. Input-output definitions of ADM1 process

In order to ensure an efficient operation, the organic loading of the influent should be continuously adapted to the treatment capacity of the digester. In the situation that the system operates below its capacity, one refers to this operating point as *underload*. An organic *overload* causes a drop in the pH level and can stop the microbiological conversion, therefore stopping the methane production. From the point of view of control, an increase in the biogas production with a decrease in the methane production can be used as an indicator that the *overload* phase is triggerred.

III. ANALYSIS OF THE SYSTEM

A. Static Characteristic

It is assumed that the flow rates of the input streams are physically bounded in the range [0;500]($\frac{m^3}{d}$). In order to determine the treatment capacity of the system and the operational constraints of the two inputs, the behaviour of the ADM1 was simulated for a constant feed over 100 days with each pair of input values varied with a constant step of 50 m^3/d in the given range (i.e. a staircase excitation signal varying from min. to max. applicable input rates). The corresponding steady state values of the biogas flow rate for different operating points in the physical range are given in Fig. 3 below. Similarly, Fig. 4 depicts the static characteristic for the methane concentration.

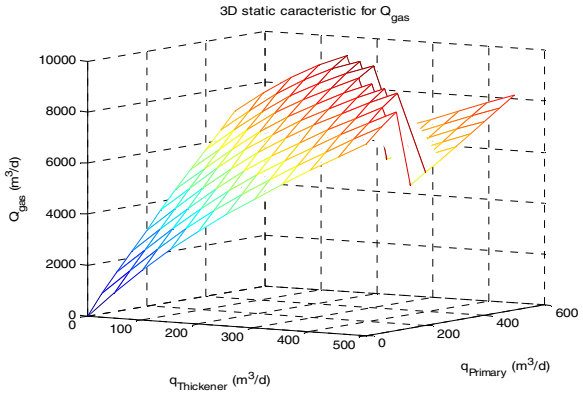

Figure 3. Static characteristic for biogas flow rates as a function of the two inputs.

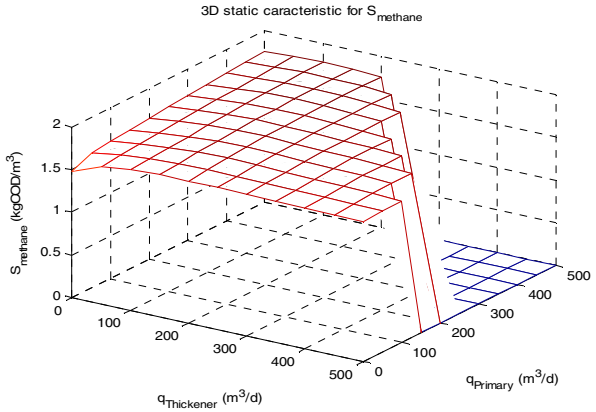

Figure 4. Static characteristic for the methane concentration as a function of the two inputs.

By increasing the input flow rates, both biogas flow rate and methane concentration increase. Hence, the system is underloaded until a maximum limit is reached, i.e. the maximum treatment capacity. By increasing any of the input flow rates over these limits, the methane concentration drops down followed by a decrease with a smoother slope in biogas flow rate. In this case the system is overloaded. The pairwise values where the methane concentration is maximal represent the operational constraints of the two inputs $(q_{Thickener};\ q_{Primary})$:{ (500; 100); (450; 150); (400; 250); (350; 300); (300; 350); (250; 450); (200; 500)}, given explicitly in Fig. 5.

Note that in Fig. 4 the methane concentration is rather flat (invariant) in a wide operating range, but then drops rapidly, while the biogas flow rate displays gradual changes according to the input values. One may conclude from this that it could be sufficient to follow up the biogas flow rate to detect process overload. However, since the methane concentration drop is followed by a decrease in the biogas flow rate, this will not be the case.

As stated before, the variable of interest is the methane production. Therefore, the optimal operating point is given by the maximum value of the product between biogas flow rate and methane concentration. The inputs can take only values within the physical and operational bounds. When determining the nominal operating point, the bounds are lowered with a constant value of $100\ m^3/d$, such that the inputs can be manipulated around the point in question (see Fig.5). According to the information extracted from the static characteristics, the methane production is optimal for the following pairwise values: $(q_{Thickener};\ q_{Primary}) = (200; 400)\ \frac{m^3}{d}$.

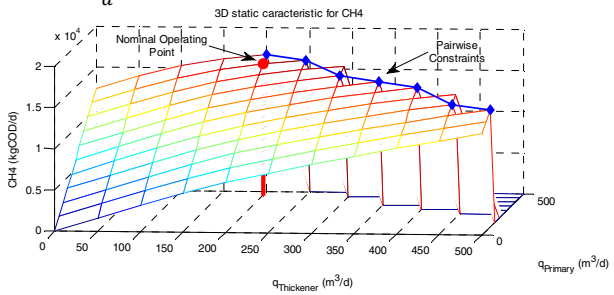

Figure 5. Steady state methane production for the operating points in the physical range, taking into account the operational constraints and the nominal operating point

B. Dynamic Step Responses

As previously described, one of the inputs is varied in the range $[0;500](\frac{m^3}{d})$ with a constant step of 50 m^3/d, while the other one is kept constant. The constant values are chosen such that the operational bounds are not exceeded. When the flow rate from the Thickener is varied, the flow rate from the Primary Clarifier is maintained at 100 m^3/d. Similarly, when the primary flow rate changes its values, the flow rate from the Thickener is kept at 200 m^3/d.

As previously shown in the static characteristics, the static gain for q_{gas} and S_{gas,CH_4} depends on the values of the two inputs. To compare the output dynamics when the inputs are varied in turn within the physical bounds, the following normalization formula has been applied to the outputs:

$$Y_{norm} = sign(U) * \frac{Y - Y_0}{|Y_\infty - Y_0|} \qquad (1)$$

where Y stands for output of the model (q_{gas} or S_{gas,CH_4}), U stands for the input of the model ($q_{Thickener}$ or $q_{Primary}$) which is being varied, Y_0 is the output initial value, Y_∞ the output steady state, $sign(U)$ the sign of the input step and Y_{norm} the normalized output. In this manner, the normalized outputs converge to +1 for a positive static gain and to -1 for a negative gain; an illustrative example is given in Fig. 6.

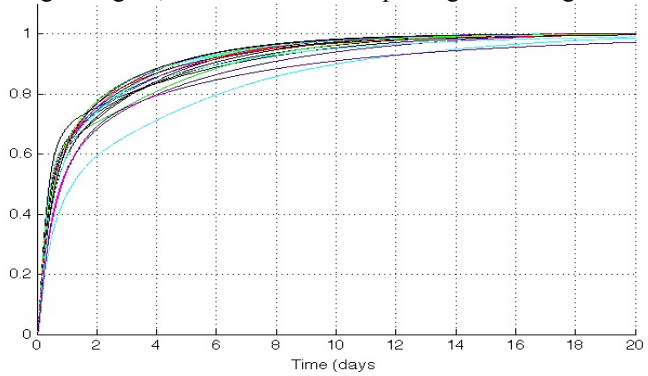

Figure 6. Normalized dynamic characteristic for the biogas flow rate when the flow from the thickener is kept constant at $200m^3/d$

The biogas flow rate, q_{gas} exhibits a positive gain when varying $q_{primary}$ (fig 6) as well as in case of varying $q_{thickener}$ (results not shown), i.e. the output increases when any of the inputs increase. The behavior of q_{gas} in relation to each of the two inputs can be modelled through a second-order model containing a fast time constant and a slow one. The identification of these models will be made around the nominal operating point, the differences between the behavior due to other input values and the obtained models will be considered as identification errors. Considering that the models will be used for the prediction of the output for a period of 5-10 days, the second- order models can be approximated by first- order models containing only the fast time constant.

From this dynamic analysis, it results that the methane concentration S_{gas,CH_4} shows distinctly two dynamic phases depending on the operating point (i.e. the pair of input values). It either has a positive gain and a non-minimum phase zero, or presents a negative gain and overshoot. Given this behavior, it is proposed to make use of simplified second-order models, identified around the nominal operating point to study the feasibility of applying model-based predictive control for the optimization of methane production. In this way, we assume that the modeling errors are handled by the control strategy.

The ADM1 reactor volume combined with the influent flow rate results in the SRT (sludge retention time) =HRT (hydraulic retention time, equal to SRT since the tank is perfectly mixed) =V/(Qprim+Qsec)= 19 days.

IV. Identification and Model Validation

A fairly general form for a *n*-th order model can be briefly expressed by the following formula [13]:

$$y(t) = \theta^T * \Phi(t) \qquad (2)$$

where

$\theta = [a_1\ a_2 \dots\ a_{n_a}\ b_0\ b_1 \dots\ b_{n_b}]^T$ is the parameter vector, and

$\Phi(t) = [-y(t-1)\ -y(t-2)\ \dots\ -y(t-n_a)\ u(t-d\ ut{-}d{-}1 \dots\ ut{-}d{-}nb]T$

is the measurement vector; *t* is the discrete time index, n_a and n_b are the orders of the transfer function polynomials and *d* is the time delay index.

Such a simple, linear model can represent only an approximation of a real process, which is subjected to disturbances that cannot be avoided. Between the output of the process and the output of the model exists always an error $\varepsilon(t)$. The basic idea of the Prediction Error Method consists in the calculation of the parameter vector such that this error is as small as possible. One of the most used ways to minimize the error $\varepsilon(t)$ is to consider the sum of squared residuals. In this case the cost function that is minimized is:

$$J(\theta) = \varepsilon^T * \varepsilon \qquad (3)$$

The test signal applied for identification is the pseudo-random binary sequence (PRBS) which switches its values between $+50\ m^3/d$ and $-50\ m^3/d$ at certain intervals that are integer multiples of $T_e = 2\ days$. The specified period ($T_e = 2\ days$) gives the smallest pulse length in the PRBS signal. In order to get a good identification for the static gain, at least one of the pulses in the sequence has to present a length equal or higher than the rise time of the process. Therefore, the pulse of maximum length lasts *D= 20* days. The number of samples of this pulse, $n = \frac{D}{Te} = 10$, considering T_e as the sampling time of the PRBS, gives the period of the test signal: $L = (2^n - 1) * T_e = 2046\ days$.

The signal thus obtained is added to the value corresponding to the nominal operating point for each of the inputs while the other one is kept constant at the value given by the point in question. The process outputs lowered with the steady state values of the outputs obtained for the nominal operating point and the PRBS are used for the model identification by Prediction Error Method. The identified transfer functions are:

$$G_{11}(s) = \frac{q_{gas}(s)}{q_{Thickener}(s)} = 31.9211\,\frac{s+0.2034}{(s+3.4432)(s+0.18)} \qquad (4)$$

$$G_{12}(s) = \frac{S_{gas,CH_4}(s)}{q_{Thickener}(s)} = -0.0012\,\frac{s+0.1513}{(s+2.6413)(s+0.2571)} \qquad (5)$$

$$G_{21}(s) = \frac{q_{gas}(s)}{q_{Primary}(s)} = 17.4238\,\frac{s+0.4819}{(s+2.998)(s+0.2756)} \qquad (6)$$

$$G_{22}(s) = \frac{S_{gas,CH_4}(s)}{q_{Primary}(s)} = 6.9987 * 10^{-4}\,\frac{s-0.0248}{(s+1.8415)(s+0.2352)} \qquad (7)$$

Figures 7-10 depict the validation of the identified models representing the four transfer functions for the two-input two-output (TITO) system.

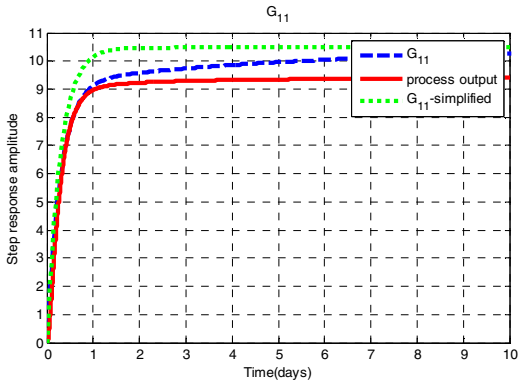

Figure 7. Step response and validation of $G_{11}(s)$

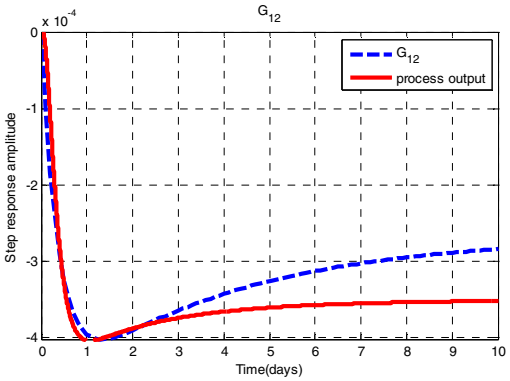

Figure 8. Step response and validation of $G_{12}(s)$

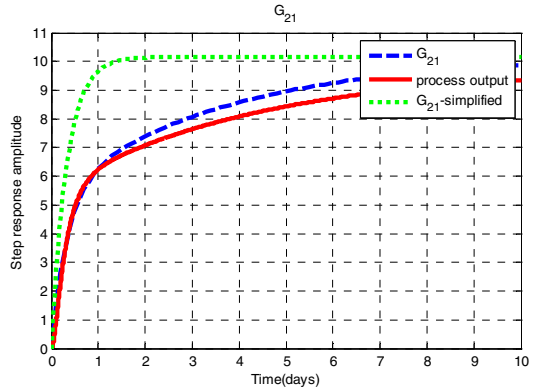

Figure 9. Step response and validation of $G_{21}(s)$

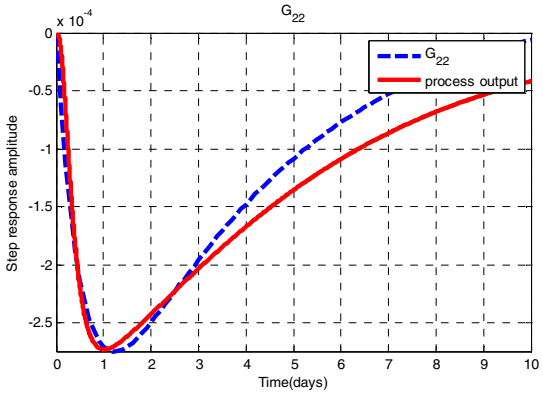

Figure 10. Step response and validation of $G_{22}(s)$

The models obtained are second-order transfer functions containing two real poles and a zero. G_{11} and G_{21} exhibit a positive gain, a fast and a slow time constant and a zero value close to the smallest pole, as shown in the relations (4) and (6). Hence, the two transfer functions for the biogas flow rate q_{gas} can be approximated by a first-order transfer function that includes only the static gain and the fastest time constant. G_{12} and G_{22} show the two behaviors of the methane concentration S_{gas,CH_4}, one presenting a negative gain (5) and the other a non-minimum phase zero (7).

For the model validation, one step of 50 m^3/d has been applied on each of the inputs around the nominal operating point. In order to get the unit step response, the obtained outputs were divided by the input step size and then plotted on the same figure with the step response of the corresponding transfer function.

As we may observe from the step responses given in the figures 7-10, the identification error is small during the transient state and increases while moving towards the steady state due to inaccuracy in model's static gain. Such an approach is suited to predictive control strategies, where the outputs are predicted on a limited prediction horizon; the steady state error is intrinsically removed by the controller.

V. Predictive Control: EPSAC

In this paper, we apply the EPSAC (Extended Prediction Self-Adaptive Control) strategy described in detail in [8]. The EPSAC-MPC is based on a generic process model:

$$y(t) = x(t) + n(t) \tag{8}$$

The disturbance $n(t)$ includes the effects in the measured output $y(t)$ which do not come from the model input $u(t)$ via the available model. These non-measurable disturbances have a stochastic character with non-zero average value, which can be modeled by a colored noise process:

$$n(t) = \left[C(q^{-1}) / D(q^{-1}) \right] \cdot e(t) \tag{9}$$

with: $e(t)$ - uncorrelated (white) noise with zero mean value; $C(q^{-1})$ and $D(q^{-1})$ - monic polynomials in the backward shift operator q^{-1} of orders n_c and n_d. The disturbance filter $C(q^{-1})/D(q^{-1})$ is defined as a pure integrator so that the steady state error is zero.

The relationship between $u(t)$ and $x(t)$ is given by the generic dynamic system model:

$$x(t) = f\left[x(t-1), x(t-2), \cdots, u(t-1), u(t-2), \cdots \right] \tag{10}$$

In the setup of the ADM1, $x(t)$ represents the output of the prediction models (4)-(7). The noise $n(t)$ represents all differences between the actual plant output from ADM1 and the predicted output from the identified models (4)-(7).The process output is predicted at time instant t over the prediction horizon N_2 based on the measurements available at that moment and the future outputs of the control signal. The predicted values of the output are:

$$y(t+k \mid t) = x(t+k \mid t) + n(t+k \mid t) \tag{11}$$

Prediction of $x(t+k|t)$ and of $n(t+k|t)$ can be done respectively by recursion of the process model and by using filtering techniques on the noise model (9) [8].

In the EPSAC control strategy, the future response is considered as being the cumulative result of two effects:

$$y(t+k/t) = y_{base}(t+k/t) + y_{opt}(t+k/t) \tag{12}$$

where $y_{base}(t+k/t)$ represents:

- effect of past control $\{u(t\text{-}1),\ u(t\text{-}2),\ \ldots\}$ (initial conditions at time t);
- effect of a *base* future control scenario, called $u_{\text{base}}(t+k \mid t),\ k \geq 0$, which is defined *a priori*; for linear systems the choice is irrelevant, a simple choice being $\{u_{\text{base}}(t+k \mid t) \equiv 0,\ k \geq 0\}$;
- effect of future (predicted) disturbances $n(t+k|t)$.

and $y_{opt}(t+k/t)$ represents:

- effect of the *optimizing* future control actions $\{\delta u(t \mid t),\ \delta u(t+1 \mid t),\ \ldots\ \delta u(t+N_u-1 \mid t)\}$ with $\delta u(t+k \mid t) = u(t+k \mid t) - u_{\text{base}}(t+k \mid t)$. The *design* parameter N_u, called the *control horizon* (a well-known concept in MPC-literature), is considered in this paper equal to 1.

The controller output is obtained by minimizing:

$$J(\mathbf{U}) = \sum_{k=N_1}^{N_2} \left[r(t+k/t) - y(t+k/t) \right]^2 \qquad (13)$$

where *r(t+k/t)* is the desired *reference trajectory*. The controller output is obtained by minimizing a cost function. The cost function (13) is a quadratic form in **U,** having the following structure:

$$J(\mathbf{U}) = (\mathbf{R} - \bar{\mathbf{Y}} - \mathbf{G} \cdot \mathbf{U})^T \cdot (\mathbf{R} - \bar{\mathbf{Y}} - \mathbf{G}\mathbf{U}) \qquad (14)$$

with **R** the reference trajectory, $\bar{\mathbf{Y}}$ and **U** defined as:

$$\bar{\mathbf{Y}} = \left[Y_{base}(t+N_1/t) ..... Y_{base}(t+N_2/t) \right]^T \qquad (16)$$

$$\mathbf{U} = \left[\delta u(t/t) ..... \delta u(t+N_u-1/t) \right]^T \qquad (17)$$

and the **G** matrix contains step response coefficients of the process model. Minimization of (14) w.r.t. **U** yields the optimal solution:

$$\mathbf{U}^* = \left[\mathbf{G}^T \cdot \mathbf{G} \right]^{-1} \mathbf{G}^T \cdot (\mathbf{R} - \bar{\mathbf{Y}}) \qquad (15)$$

Relation (15) represents the input which will be applied to the process.

VI. Performance Evaluation

In a single input single output context, we consider the flow of the thickener as the manipulated variable and the flow of gas production as the controlled variable. In order to tune the EPSAC predictive controller, by means of the prediction horizon N_2, we first investigated the effect of changing N_2 on the output flow rate. This is illustrated in Fig. 11. We can conclude that a good trade-off between control effort and output variations is made around N_2=50 samples.

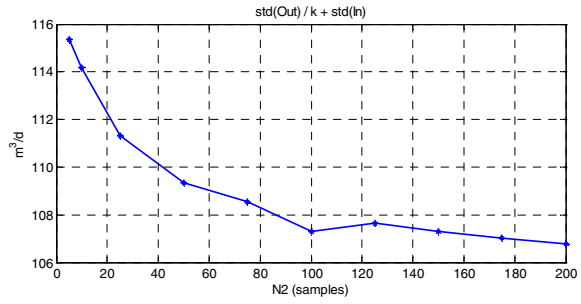

Figure 11. Evolution of the variations in the output biogas flow production with variations in the control effort as a function of the prediction horizon. One sample is 15 minutes.

To verify the added value of predictive control against open-loop control, we considered two cases. Case 1: when the input flow of the thickener is kept at a constant rate around 200 m³/d and Case 2: when the input flow is manipulated by the EPSAC control strategy. The simulation has been considered on 609 days. Figure 12 compares the result of the two strategies, where it can be observed that the open-loop control is not able to maintain the output gas flow within reasonable boundaries: it varies between 6000-10000 m³/d. By contrast, the output gas flow in the EPSAC control loop is maintained nicely within the 8000-9000 m³/d interval (setpoint=8500 m³/d). However, from a control engineering standpoint, it does not suffice to analyze only the output variable, it is necessary to look also at the control effort. The corresponding control effort is depicted in Figure 13 below. One may observe that the EPSAC control strategy has to continuously manipulate the inlet flow of the thickener to account for disturbance variations. However, on the average, the order of magnitude is fairly close to that of manual control. We can conclude that EPSAC MPC control is thus suitable to control the anaerobic digestion process within the ADM1.

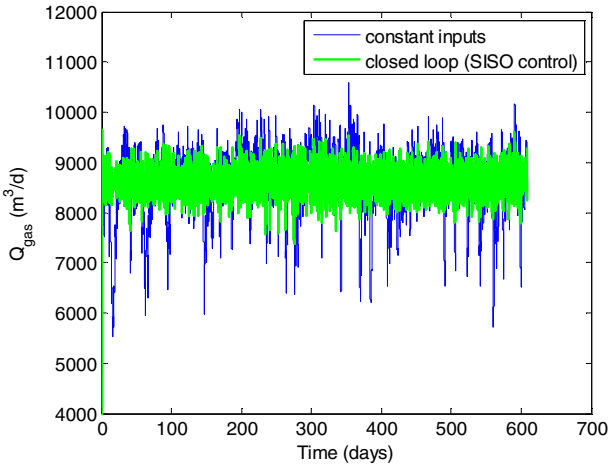

Figure 12. Output variable in case of manual control (constant input) and for EPSAC closed loop control.

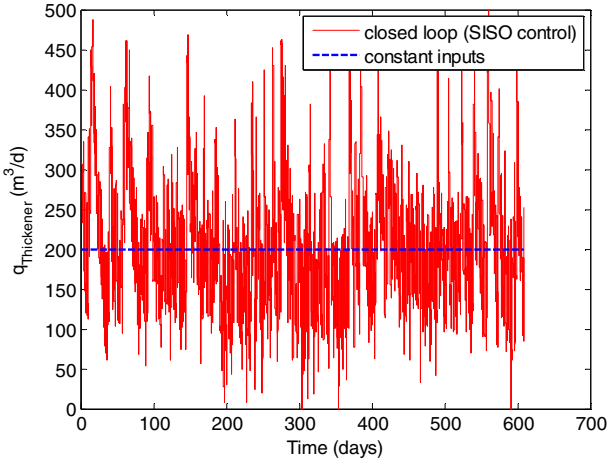

Figure 13. Control effort in manual (constant input) and closed loop control (EPSAC).

It is also important to look at the evolution of the second output, the methane concentration, for it may be influenced through the multivariable coupling effect. This is illustrated in figure 14. We can observe that no significant differences

occur between the two strategies. However, the overall objective was to maximize the methane production. This is defined as the product between the output gas flow and the methane concentration. The result is depicted in figure 15. We can conclude that the EPSAC strategy is able to maintain the methane production at a stable output production rate, where the manual control is prone to significant variations. The overview of the net production is given below (the same scenario used for both simulations): open loop: $9.2751*10^9$ kgCOD and closed loop: $9.2794*10^9$ kgCOD. The total gain in methane production due to the control strategy: 4300000 kgCOD.

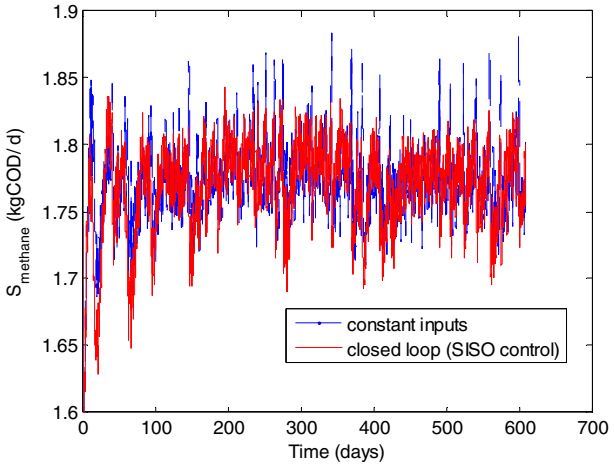

Figure 14. Evolution of the methane concentration as a result of multivariable coupling.

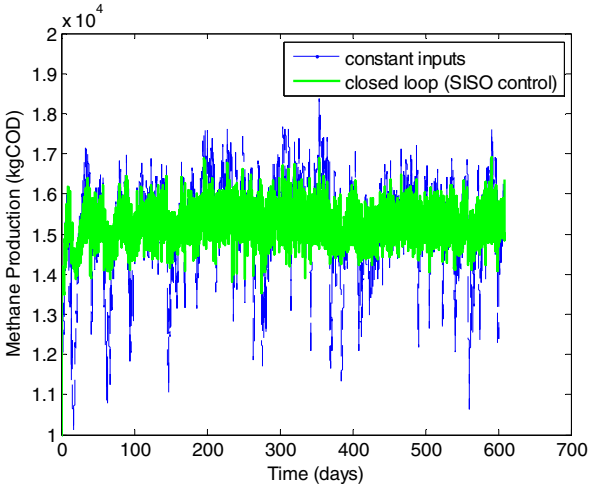

Figure 15. Evolution of the overall methane production.

VII. Conclusions and Perspectives

The results in this paper presents a first step towards the development of a fully multivariable predictive control strategy for maximizing the methane production in anaerobic digestion processes tested on the ADM1 benchmark. Based on this preliminary study, significant insight has been gathered, allowing to define operating range and constraints in the inputs-outputs of the process.

The next steps are to determine a suitable cost function to be used in the predictive control algorithm such that maximum production is ensured while satisfying stability constraints (i.e. avoid overload).

References

[1] J.P. Steyer, O. Bernard, D.J. Batstone, I. Angelidaki, "Lessons learnt from 15 years of ICA in anaerobic digesters", *Wat. Sci. Tech.*, **53**(4-5), 25-33, (2006)

[2] J.P. Steyer, P. Buffiere, D. Rolland, R. Moletta, "Advanced control of anaerobic digestion processes through disturbance monitoring", *Wat. Res.*, **33**(9), 2059-2068, (1999)

[3] M. Estaben, M. Polit, J-P. Steyer, "Fuzzy control for an anaerobic digester", *Control. Eng. Pract.*, **5**(98), 1303-1310, (1997)

[4] P. Renard, D. Dochain, G. Bastin, H. Naveau, E.-J. Nyns, "Adaptive control of anaerobic digestion processes – a pilot scale application", *Biotechnol. Bioeng.*, **31**(4), 287-294, (1988)

[5] W. Shen, X. Chen, J.P. Corriou, "Application of model predictive control to the BSM1 benchmark of waste water treatment process" *Comp. Chem. Eng.*, **32**(12), 2849-2856, (2008)

[6] V.M. Cristea, C. Pop, P. Agachi, "Model predictive control of the waste water treatment plant based on the benchmark model BSM1" ESCAPE **18**, (2008)

[7] M. Francisco, P. Vega, S. Revollar, "Model predictive control of BSM1 benchmark of wastewater treatment process: a tuning procedure", 50th IEEE CDC-ECC, Orlando, Florida, USA, 7057-7062, (2011)

[8] R. De Keyser, "A Gent-le approach to predictive control", UNESCO Encyclopaedia of Life Support Systems (EoLSS), EoLSS Publishers Co Ltd, Oxford30p, (2003), www.eolss.net

[9] D.J. Batstone, J. Keller, I. Angelidaki, S.V. Kalyuzhnyi, S.G. Pavlostathis, A. Rozzi, W.T.M. Sanders, H. Siegrist, V.A. Vavilin, "Anaerobic Digestion Model No.1 (ADM1)", IWA Scientific and Technical Report #13, IWA Publishing, London, UK, (2002)

[10] U. Jeppsson, C. Rosen, J. Alex, J. Copp, K.V. Gernaey, M.-N. Pons, P.A. Vanrolleghem, "Towards a benchmark simulation model for plant-wide control strategy performance evaluation of WWTPs", *Wat. Sci. Tech.*, **53**(1), 287-295, (2006)

[11] I. Nopens, D.J. Batstone, J.B. Copp, U. Jeppsson, E. Volcke, J. Alex, P.A. Vanrolleghem, "An ASM/ADM model interface for dynamic plant-wide simulation", *Wat. Res.*, **43**(7), 1913-1923, (2009)

[12] E.I.P. Volcke, K.V. Gernaey, D. Vrecko, U. Jeppsson, M.C.M. van Loosdrecht, P.A. Vanrolleghem, "Plant-wide (BSM2) evaluation of reject water treatment with a SHARON-Anammox process", *Wat. Sci. Tech.*, **54**(8), 93–100, IWA Publishing, (2006)

[13] L. Ljung, "System Identification - Theory for the User", Prentice-Hall, Englewood Cliffs, NJ, ISBN 0-13-881640, (1987)